

Metamorphosis of spiny lobsters (*Panulirus argus* and *Panulirus guttatus*) in the Yucatan Current as inferred from the distribution of pueruli and final stage phyllosomata

Patricia Briones-Fourzán ^{1,*} Julio Candela ² Laura Carrillo ³ Alí F. Espinosa-Magaña,^{1,4}
Fernando Negrete-Soto,¹ Cecilia Barradas-Ortiz,¹ Edgar Escalante-Mancera ¹
Rubén Muñoz de Cote-Hernández,^{1,5} Rogelio Martínez-Calderón,¹ Enrique Lozano-Álvarez ¹

¹Unidad Académica de Sistemas Arrecifales, Instituto de Ciencias del Mar y Limnología, Universidad Nacional Autónoma de México, Puerto Morelos, Mexico

²Departamento de Oceanografía Física, Centro de Investigación Científica y Educación Superior de Ensenada, Ensenada, Mexico

³Departamento de Observación y Estudio de la Tierra, la Atmósfera y el Océano, El Colegio de la Frontera Sur, Chetumal, Mexico

⁴Present address: Centro Universitario de la Costa, Universidad de Guadalajara, Puerto Vallarta, Mexico

⁵Present address: Grupo Interdisciplinario de Gestión Ambiental, A.C., Ciudad de México, Mexico

Abstract

For spiny lobsters (Palinuridae), the co-occurrence of final-stage larvae (phyllosomata) and postlarvae (pueruli) in sampling stations over oceanic waters is indicative of metamorphosis zones, some of which have been found in boundary currents. We hypothesized that metamorphosis of *Panulirus argus* and *P. guttatus* off the Mexican Caribbean coast, which has a very narrow shelf, occurs in the swift Yucatan Current (YC). During two cruises conducted in autumn 2012 and spring 2013, a mid-water trawl and a neuston net were simultaneously towed in night samplings along transects up to ~100 km across the YC. Hydrographic and current fields were derived from Conductivity, Temperature and Depth, and altimetry data. Metamorphosis occurred mainly within the YC core. However, velocity and distance to the coast of the YC varied with cruise, and features that may favor retention (a persistent coastal eddy and a countercurrent) were detected. Despite differences in size and condition of pueruli between cruises, their energy stores did not appear to decline during the shoreward migration, suggesting that metamorphosing within strong boundary currents may increase the chances of pueruli arriving more quickly to a shore. Based on previously reported current features and swimming speeds, pueruli metamorphosing up to 12 km offshore are more likely to reach the Mexican Caribbean coast without much loss of energetic reserves. This could also occur for some pueruli metamorphosing up to 30 km offshore if encountering the features favoring retention. In contrast, pueruli metamorphosing > 30 km offshore are more likely to be carried into the Gulf of Mexico and elsewhere.

Spiny lobsters (Crustacea: Decapoda: Achelata: Palinuridae) are an important component of tropical and subtropical benthic communities and constitute valuable fishing resources wherever they occur (Briones-Fourzán and Lozano-Álvarez 2013). These lobsters have a peculiar type of planktotrophic larva, known as “phyllosoma” (from the Greek “leaf-shaped body”), which develops in oceanic waters over an exceptionally long period (> 5 months). The lengthy larval duration confers these lobsters a great potential for dispersal (Phillips et al. 2006a). The final phyllosoma undergoes a complete metamorphosis into the

postlarva, known as “puerulus,” which is morphologically like an adult lobster but is completely transparent. Importantly, pueruli do not feed (Lemmens 1994), that is, they constitute a secondary lecithotrophic phase in the life cycle of spiny lobsters (McWilliam and Phillips 1997). After metamorphosis, the puerulus actively swims toward the shore, where it settles in shallow coastal habitats and begins its benthic life.

The Caribbean spiny lobster *Panulirus argus* (Latreille, 1804) and the spotted spiny lobster *Panulirus guttatus* (Latreille, 1804) co-occur throughout the wider Caribbean region. The former sustains valuable fisheries across the region, whereas the latter is a much less important resource due to its smaller size and habitat specialization. Although both species reproduce year-round, *P. argus* exhibits a major reproductive peak in spring and a minor peak in autumn (Padilla-Ramos and

*Correspondence: briones@cmarl.unam.mx

This is an open access article under the terms of the Creative Commons Attribution License, which permits use, distribution and reproduction in any medium, provided the original work is properly cited.

Briones-Fourzán 1997), whereas *P. guttatus* shows a decrease in reproductive activity during late summer (Briones-Fourzán et al. 2013). The larval phase of *P. argus* comprises 10 phyllosoma stages, with an estimated duration of 5–9 months (Goldstein et al. 2008), and the puerulus of this species is rather small (~6 mm carapace length [CL] on average) (Martínez-Calderón et al. 2018). Upon reaching the shore, the pueruli of *P. argus* settle in shallow marine vegetated habitats in reef lagoons or shallow bays, where the juveniles remain for several months before migrating to the subadult/adult habitats (coral reefs). In *P. guttatus*, Baisre and Alfonso (1994) described phyllosoma stages VI to X from wild-caught specimens and considered stage X to be the penultimate stage. Goldstein et al. (2019) cultured *P. guttatus* larvae from eggs and although they failed to obtain the final phyllosoma (which they considered to be the stage X), they estimated the duration of the complete larval phase in slightly over 1 yr. Compared to *P. argus*, pueruli of *P. guttatus* are much larger (~10 mm CL, Briones-Fourzán and McWilliam 1997) and settle directly in the coral reef habitat, where individuals remain for the duration of their benthic life (Briones-Fourzán and Lozano-Álvarez 2013).

Because the nonfeeding pueruli have limited energetic reserves (Fitzgibbon et al. 2014), the probability of a puerulus to arrive to the coastal settlement habitats could depend to a great extent on the distance to the coast where it metamorphosed as well as on the local hydrography. Therefore, there has been much debate as to where metamorphosis of spiny lobsters takes place (reviews in Phillips et al. 2006a; Phillips and McWilliam 2009). Catches of phyllosomata metamorphosing into pueruli undoubtedly indicate the location of metamorphosis zones, but such catches are very rare (Yoshimura et al. 1999) because the entire metamorphosis molt takes about 10 min on average (Murakami et al. 2007). Therefore, in general, sea regions in which final phyllosomata and pueruli are found together in the same individual sampling stations have been considered metamorphosis zones. Based on this criterion, several palinurids species have been found to metamorphose in oceanic waters beyond the shelf break (Phillips and McWilliam 2009). Metamorphosis of *Panulirus cygnus* appears to be related with the Leeuwin Current—an anomalous eastern boundary current of warm, low-salinity water that flows southward along the coast of Western Australia (Griffin et al. 2001; Waite et al. 2007)—but also with the internal margins of anticyclonic eddies, which are frontal zones rich in potential food for phyllosomata (Phillips and McWilliam 2009; Wang et al. 2014). In New Zealand, the distribution of newly metamorphosed pueruli of *Jasus edwardsii* followed the inshore margins of the Wairarapa eddy fields (Jeffs et al. 2001), adjacent to the stronger southward flow of the East Cape Current (Chiswell and Booth 2005), whereas in Japan, metamorphosis of *Panulirus japonicus* mainly occurred within the Kuroshio Current, a strong western boundary current (Yoshimura et al. 1999; Sekiguchi and Inoue 2002; Inoue

and Sekiguchi 2009). This information strongly suggests that metamorphosis of palinurids is associated with strong boundary currents.

To our knowledge, no studies have attempted to determine the oceanic zones where metamorphosis of *P. argus* or *P. guttatus* occurs. In general, previous studies on the distribution of phyllosomata in the wider Caribbean region have been based on samples obtained in plankton nets of relatively small dimensions (mouth aperture: $\leq 1 \text{ m}^2$ and/or mesh size: 0.33–1 mm) towed at rather low speeds ($\leq 0.5 \text{ m s}^{-1}$) (Richards and Pothoff 1981; Manzanilla-Domínguez and Gasca 2004; Canto-García et al. 2016). Such nets filter a relatively small volume of water and hence are not adequate to sample late-stage phyllosomata or pueruli, which are highly dispersed in oceanic waters (Phillips et al. 2006a). Also, pueruli are fast swimmers and can avoid slow-moving nets (Phillips and Olsen 1975; Calinski and Lyons 1983; Jeffs et al. 2005). Appropriate sampling of these organisms requires filtering larger volumes of water, for example, using nets of greater dimensions and larger mesh sizes to be towed at faster speeds ($> 1 \text{ m s}^{-1}$) (Yoshimura et al. 1999; Dennis et al. 2001; Jeffs et al. 2001). Obtaining hydrographic data at the same time as larval sampling can provide further insight into the zones of metamorphosis (Chiswell and Booth 2005; Phillips and McWilliam 2009).

In the western Caribbean Sea, the Yucatan Current (YC) is a dominant oceanic feature. It is one of the strongest and most dynamically active western boundary currents in the world, with an average velocity of 1 m s^{-1} and magnitudes of up to 3 m s^{-1} prior to its passage through the Yucatan strait. This current variability appears to be strongly influenced by the passage of eddies through the region (Candela et al. 2003; Cetina et al. 2006; Carrillo et al. 2015). In the present study, we tested the hypothesis that metamorphosis of *P. argus* and *P. guttatus* occurs within the YC. For this, we conducted an intensive sampling of late stage phyllosomata and pueruli using nets with large mesh sizes and obtained hydrographic data to determine the location of the current, the cross-section geostrophic flow velocities, and the surface geostrophic current field. For *P. argus* pueruli, we also quantified several biochemical variables to test for a potential decrease in energy reserves during their shoreward migration.

Materials and methods

Study area

The study area covered ~30,500 km² of oceanic waters off the eastern coast of the Yucatan Peninsula, between the Yucatan channel to the north and the Bays of Ascensión and Espíritu Santo to the south (Fig. 1). This area, located in the western Caribbean Sea, is characterized by the YC, which flows parallel to the shore in a SW–NE direction, and an abrupt bathymetry with depths rapidly falling below 200 m a few kilometers from the shore (Cetina et al. 2006; Carrillo et al. 2015). According to Phillips and McWilliam (2009),

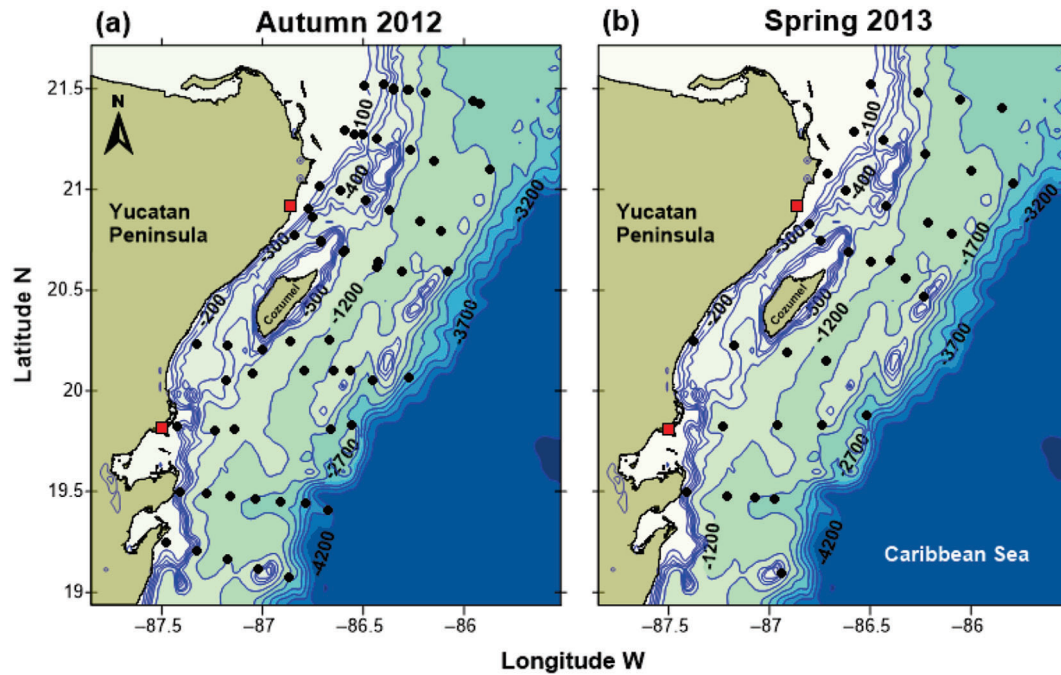


Fig 1. Study area, showing location of plankton sampling stations (black dots) during (a) the autumn 2012 cruise and (b) the spring 2013 cruise. The red squares denote the coastal locations where recently settled pueruli of *Panulirus argus* were obtained from artificial subsurface collectors in the same seasons and years.

metamorphosis of palinurids probably occurs within ~ 100–150 km of the shelf break; therefore, we established an array of sampling stations following transects perpendicular to the shelf break. Distance of sampling stations to the shore varied from 2 to 100 km over depths ranging between 35 and 2700 m; however, given that the continental shelf is very narrow (< 3 km) along a great part of the coast (Briones-Fourzán et al. 2008), virtually all stations were beyond the shelf break, that is, over depths greater than 200 m (Fig. 1).

Collection of organisms

Based on the interannual seasonal settlement pattern of *P. argus* pueruli which shows a major settlement peak in autumn and a secondary, smaller peak in spring (Briones-Fourzán et al. 2008), we conducted two oceanographic cruises using UNAM's R/V *Justo Sierra*: one in the autumn of 2012 (14–24 November) and the other one in the spring of 2013 (10–20 April). Hereafter, these cruises will be referred to as the autumn 2012 cruise and the spring 2013 cruise, respectively. In the coastal habitats, settlement of pueruli peaks around the dark phase of the moon (Briones-Fourzán 1994), whereas at sea, late stage phyllosomata and pueruli rise closer to the ocean surface in dark nights (Ritz 1972; Phillips et al. 1978; Bradford et al. 2005). Therefore, both cruises were planned to be carried out during the dark moon phase (i.e., between the dates of the last and first quarters, including the new moon). This was accomplished in the spring cruise, but the autumn cruise was delayed 1 week for reasons beyond our control

(a delay in the ship's maintenance schedule) and had to be conducted between the dates of the new moon and the full moon.

Two nets were simultaneously used in each sampling station: a large mid-water Tucker trawl (effective mouth area: 9 m²; length: 12 m; mesh size: 10 mm) and a smaller neuston net (mouth area: 1.5 m²; length: 3 m; mesh size: 3 mm) (Lozano-Álvarez et al. 2015). The Tucker trawl was towed from stern at depths of 5–15 m and was fitted with a Sea-Bird SBE39 data logger to record time, depth, and temperature during the tow. The neuston net was towed from starboard approximately mid-ship, within the uppermost meter of the water column. To increase the chances of catching larvae, all larval samplings were done during the hours of darkness (between 1 h after sunset and 1 h before sunrise). The nets were towed against the prevailing current at an average speed of 2.5 knots (1.3 m s⁻¹) for 30–35 min to reduce the chances of the fast-swimming pueruli (7–10 cm s⁻¹, Calinski and Lyons 1983) avoiding the nets.

Upon retrieving the nets, the cod-end was removed and the fresh plankton was immediately examined for phyllosomata and pueruli. The nets were also examined for tangled larvae. The neuston net occasionally collected large masses of floating *Sargassum* algae; these algal masses were transferred into a large container and thoroughly examined for phyllosomata and pueruli. For *P. argus*, larvae and postlarvae were identified and staged based on Goldstein et al. (2008). For *P. guttatus*, phyllosomata were

identified and staged based on Baisre and Alfonso (1994), and pueruli were identified based on Briones-Fourzán and McWilliam (1997). To test for seasonal variations in size of pueruli (Martínez-Calderón et al. 2018), all pueruli were individually photographed next to a reference measure under a stereoscopic microscope to estimate their CL using image processing software (ImageJ v.1.49) (Rasband 2015). For each species, CL of pueruli was compared between cruises with a one-way ANOVA using a General Linear Model approach (Rutherford 2001).

Hydrographic conditions and geostrophic flow velocities

To determine the hydrographic conditions and the location of the core of the YC, water temperature ($^{\circ}\text{C}$) and salinity were measured (to a depth of 500 m) using a Sea-Bird[®] SBE9/11Plus CTD system. For operational reasons, CTD profiles were carried out during the day along the same transects in which larval sampling took place during the night, but not necessarily the same stations (Fig. 2). The data processing was based on the standard routines and procedures proposed by the Sea-Bird Electronic Company using the software SEASOFT Win-32. Cross-section geostrophic flow velocities were obtained using hydrographic data

referred to the isopycnal $\sigma\text{-}t$ 27.0 kg m^{-3} as in Carrillo et al. (2016).

Surface geostrophic current fields

The surface geostrophic current field was derived from satellite-obtained sea surface dynamic altimetry data obtained from the Archiving, Validation, and Interpretation of Satellite Oceanographic data (AVISO) for the periods during which the cruises were conducted. Since currents in areas close to the coast cannot be well resolved using dynamic altimetry data, satellite observations were complemented with direct current observations for filling in the coastal gap where the satellite product is deficient, as well as to validate the satellite-derived current product in places further away from the coast. Direct current observations at ~ 60 m depth were obtained from Acoustic Doppler Current Profilers moored at four points along the YC: two of them close to the coast (~ 15 km) in Chinchorro Channel to the south and Cozumel Channel to the north, and two at a distance of ~ 50 km from the coast, one to the east of Banco Chinchorro in the south and the other north-eastward of Cozumel Island (black stars in Fig. 2). Even though the direct currents are measured at 60 m depth, the good relationship with satellite derived products

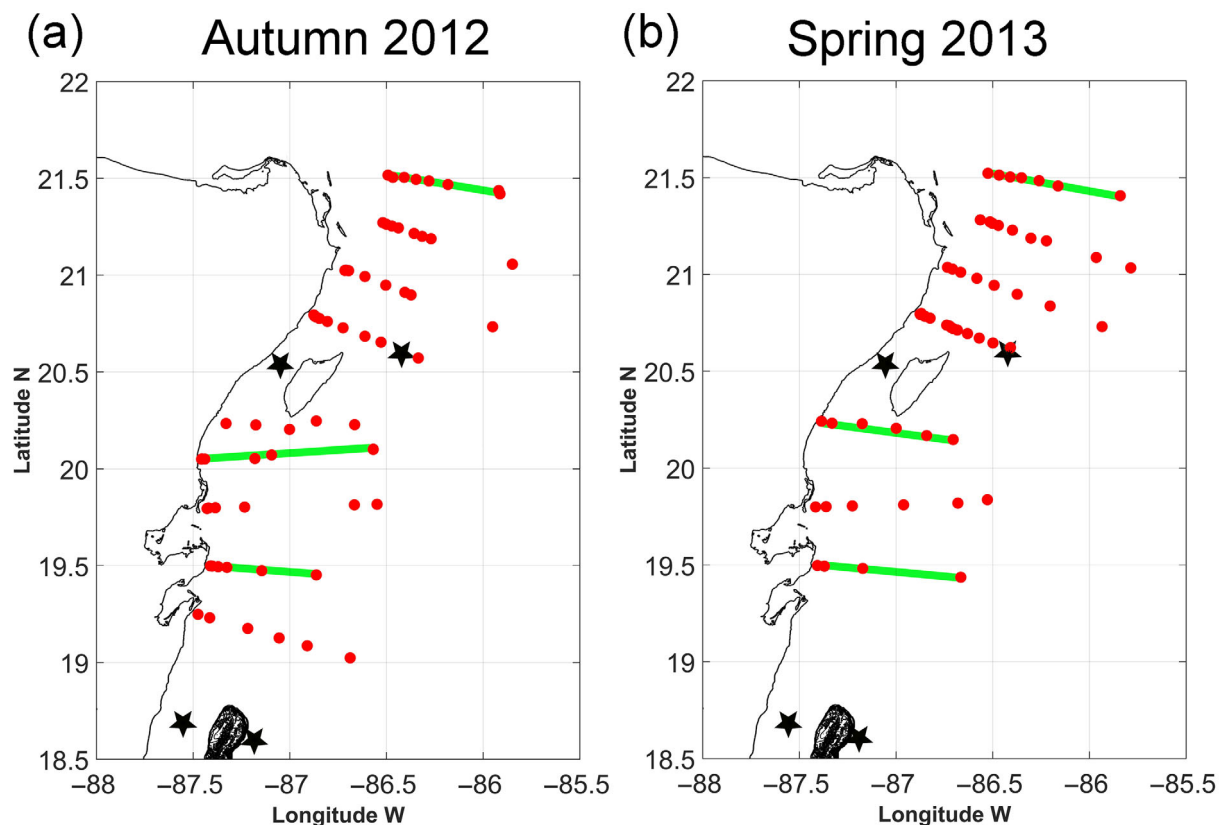


Fig 2. Location of CTD sampling stations (red dots) during (a) the autumn 2012 cruise and (b) the spring 2013 cruise. The green lines denote the transects used to analyze the cross-sectional distribution of temperature, salinity, and geostrophic flow velocity at the northern, central, and southern sections of the study area. The black stars denote the location of the four moored ADCPs current profilers for direct current observations.

(especially at the two locations distant to the coast) is indicative of the intensity of the current in the upper water column even at appreciable depths.

Estimation of larval and postlarval densities

Larval counts were standardized to larval density (number per 1000 m³). The nets were initially fitted with flow meters; however, the flow meters fitted to the midwater trawl were lost early in the autumn cruise. Also, the presence of *Sargassum* in surface waters occasionally resulted in entanglement of the algae in the rotor of the flow meter fitted to the neuston net, precluding its use to calculate the volume of water sampled. Therefore, we discontinued the use of flow meters and estimated the filtered volume (V) with the equation $V = D \times A$, where D is distance traveled, derived from the ship's speed (m s⁻¹) during the tow \times duration of the tow (s), and A = net mouth effective area (9 m² for the mid-water trawl, 1 m² for the neuston net because approximately one-third of the mouth of the neuston net remained above the ocean surface during the tows. For each species, we considered as potential metamorphosis zones those sea areas in which final phyllosomata and postlarvae were found together in the same individual sampling stations (Phillips and McWilliam 2009).

Analyses of energy reserves in pueruli of *P. argus*

To test for a potential decrease in energy reserves of pueruli across the full range of distances to the coast of our sampling stations (Phillips et al. 2006b), we subjected 52 pueruli of *P. argus* from the autumn cruise and 25 from the spring cruise to biochemical analyses. These pueruli were selected from collections obtained in stations spanning the full range of distances, that is, between 99.3 and 2.1 km from the shore. For these analyses, we also included a few transparent pueruli (six in autumn and four in spring) obtained in artificial subsurface collectors deployed about 300 m from the shore (see Fig. 1), to have data from pueruli already settled after having completed their migration from offshore waters. The pueruli were freeze-dried immediately after collection. Sample processing was as in Espinosa-Magaña et al. (2018). Briefly, pueruli were lyophilized and weighed (dry weight [DW] in mg) at the laboratory. Total lipid (TL) was determined by gravimetry from each lyophilized puerulus using the chloroform/methanol/water extraction technique of Folch et al. (1957), modified by Bligh and Dyer (1959) for small organisms (Jeffs et al. 2001). Total protein (TP) was determined by spectrophotometry using the Micro BCA Protein Assay kit and the Multiskan Spectrum plate reader (Thermo Scientific) based on the bicinchoninic acid determination method for protein (Walker 1994). For all individuals examined, we obtained DW, TL, and TP (the absolute amount of lipid [or protein], in mg, determined for each individual); TL (or TP) percentage (the percentage of lipid [or protein] relative to the DW of each individual), and DW/CL (a morphometric condition factor) (Espinosa-Magaña

et al. 2018). We used analyses of covariance (ANCOVAs) to compare each variable between cruises (categorical factor with two levels: autumn and spring), considering the distance to the shore as a continuous covariate.

Results

Hydrographic conditions and geostrophic flow velocities

Temperature and salinity fields for both cruises were analyzed along three transects, one at the northern section (close to the Yucatan Channel), one at the central section (south of Cozumel Island), and one at the southern section of the sampling area (Bahía Espíritu Santo) (Fig. 2). The hydrographic profiles show the upper water masses as defined by Carrillo et al. (2016): Caribbean Surface Water (CSW), North Atlantic Subtropical Underwater (SUW), and Tropical Atlantic Central Water (TACW).

The shape of isotherms and isohalines differed along the coast and between cruises (Figs. 3, 4, respectively). Upwelling in the northern section was observed, as there was uplifting of the thermocline (Fig. 3a,d), with the SUW reaching a depth of 25 m in autumn 2012 and 20 m in spring 2013. Deeper waters also showed a deeper location of the thermocline at about 100 m. The warmer waters of the CSW were deeper in the central (Fig. 3b,e) and southern sections (Fig. 3c,f) than in the northern section, particularly in the spring cruise. However, in the autumn cruise, the central and southern profiles showed a dome-like shape of the isotherms (Fig. 3c,e), indicating a shallower thermocline (50–75 m). The isohalines (Fig. 4) had a similar shape as the isotherms. In both cruises, the salinity field showed the maximum salinity (> 36.5) in the SUW, with a maximum core offshore, whereas the upper CSW showed some patchiness, with values < 36.1. There was also a reduction in salinity below the SUW, corresponding to the TACW (Fig. 4).

Estimates of geostrophic flow velocity of cross-sections showed that the YC extended to a depth of 200–250 m in both cruises (Fig. 5), but the location of the YC core was considered to be where the maximum speed was observed, with estimated values of 1.4 m s⁻¹ near the surface (the upper 100 m). The YC core was well defined in both cruises. However, there were clear differences between cruises, such as the relative closeness to the coast of the YC core and the presence of a coastal countercurrent (CC). Also, the location, depth, width, and speed of the YC core and CC varied between cruises and along the coast. In both cruises, the YC core was closer to the coast in the northern section than in the central and southern sections, but in the northern and southern sections it was closer to the coast in the autumn cruise (Fig. 5a,c) than in the spring cruise (Fig. 5d,f). However, during the autumn cruise the southern section (Fig. 5c) was shorter by ~ 20 km from the one in the spring cruise (Fig. 5f) and could be missing the YC core that appeared to be further offshore based on altimetry (see Fig. 6a–c). If this was the case, then the intense current feature close to the coast along this southern section (Fig. 5c) could be interpreted as a small cyclonic eddy (~ 50 km in diameter), which

is also supported by the domed shaped temperature and salinity distributions along this section (see Figs. 3c, 4c). This feature was also present, but with minor intensity and size, during the spring cruise, when the YC core was slightly divided into two in the northern section.

In both cruises, a CC appeared south of Cozumel in the central section (Fig. 5b,e). The CC was more evident in the autumn cruise, when it reached 120 m in depth and 25 km in width, and an estimated speed of up to 0.6 m s^{-1} . In the southern section, the velocity fields differed between

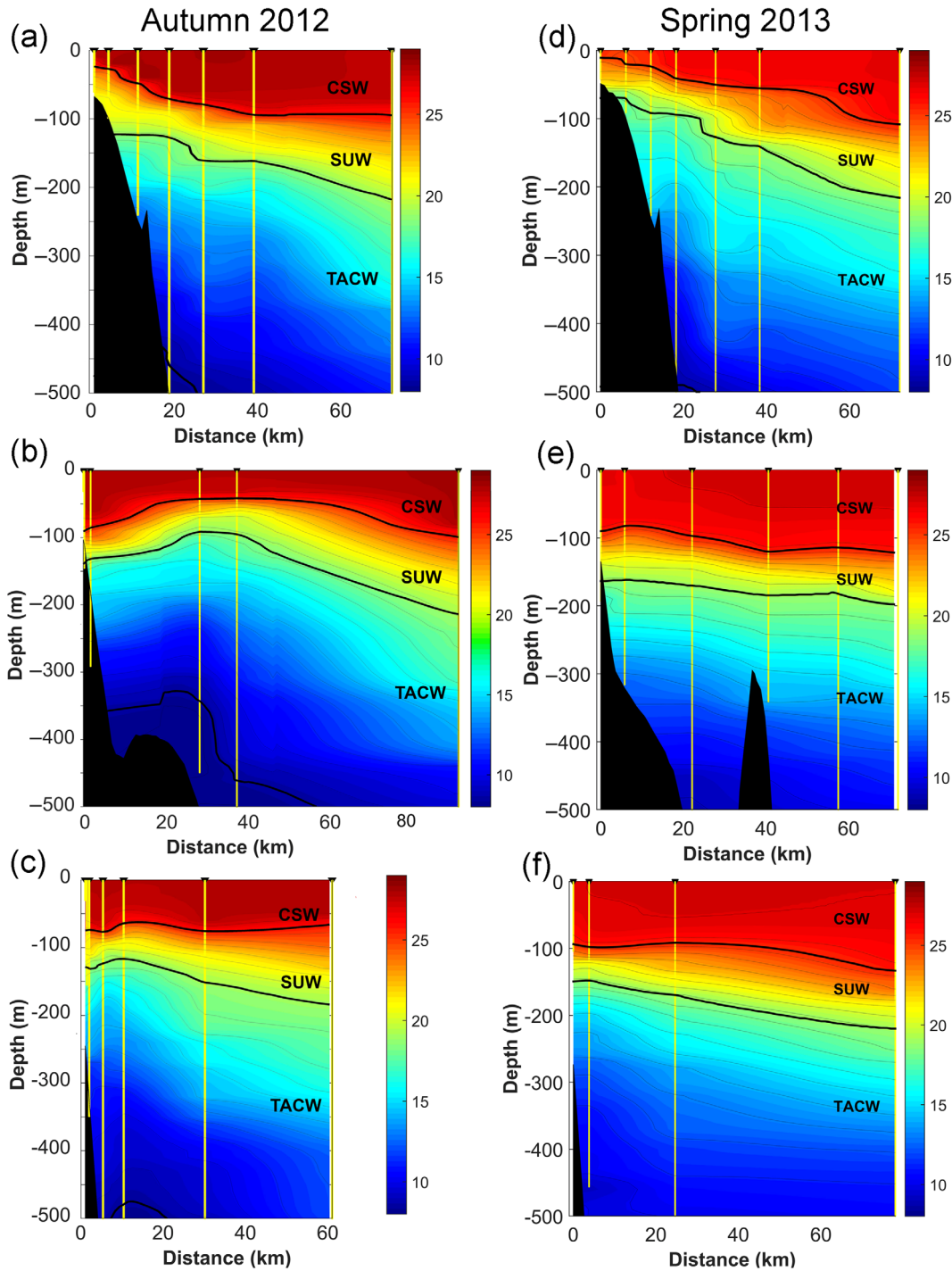


Fig 3. Cross-sectional distribution of temperature ($^{\circ}\text{C}$) between the surface and 500 m at the northern (a, d), central (b, e), and southern (c, f) sections of the study area during the autumn 2012 cruise (left column) and the spring 2013 cruise (right column). The stations are marked at the top. The thick black lines delineate water masses: CSW, SUW, and TACW.

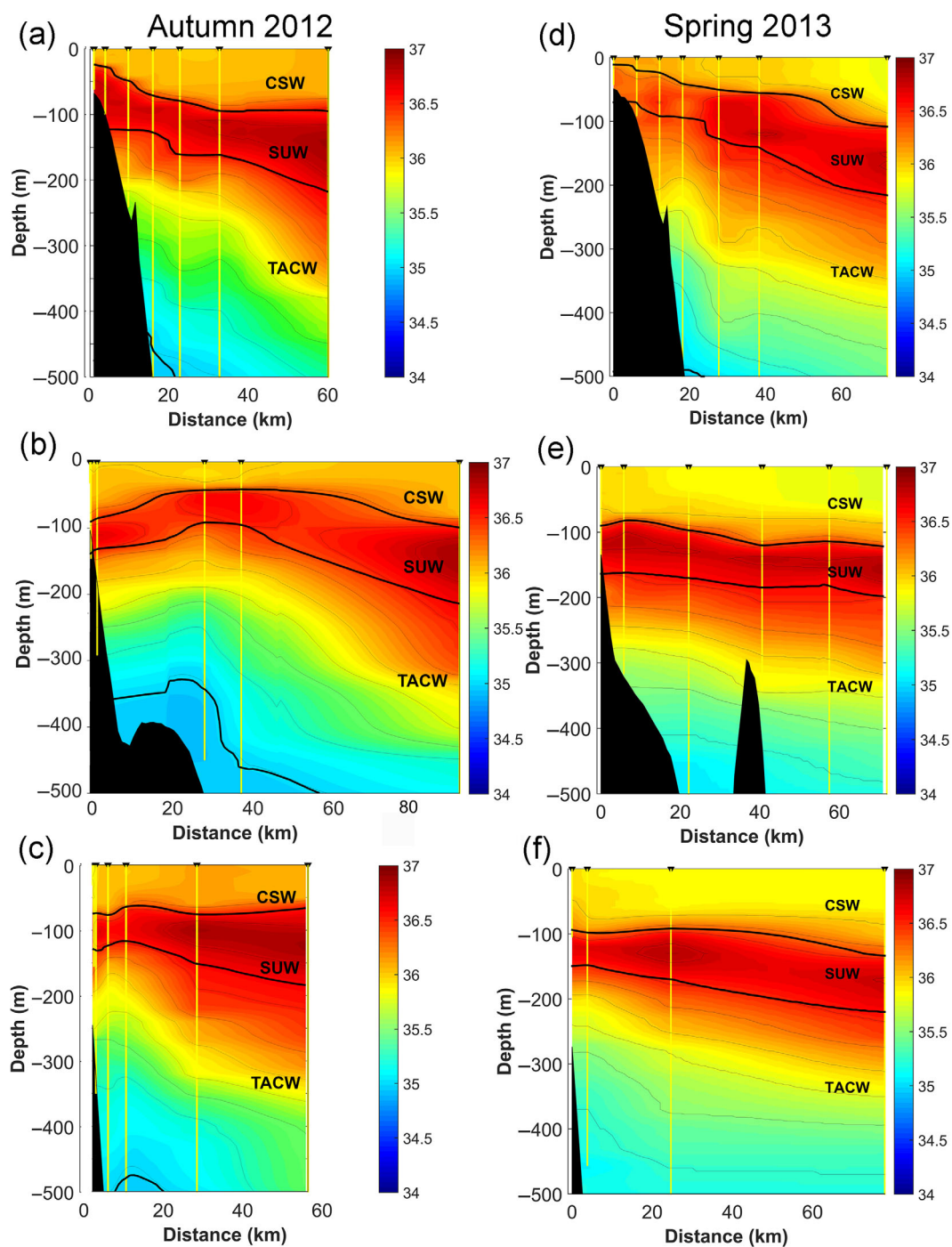


Fig 4. Cross-sectional distribution of salinity between the surface and 500 m at the northern (a, d), central (b, e), and southern (c, f) sections of the study area during the autumn 2012 cruise (left column) and the spring 2013 cruise (right column). The stations are marked at the top. The thick black lines delineate water masses: CSW, SUW, and TACW.

cruises. In the autumn cruise (Fig. 5c), there was a CC within the first 10 km from the coast and the YC core presented higher speeds (1 m s^{-1}) than during the spring cruise (0.5 m s^{-1}) (Fig. 5f).

Geostrophic current fields from altimetry measurements

Throughout each cruise, the conditions of the current field remained quite constant; therefore, the central date of each cruise was chosen to visualize the current field during that

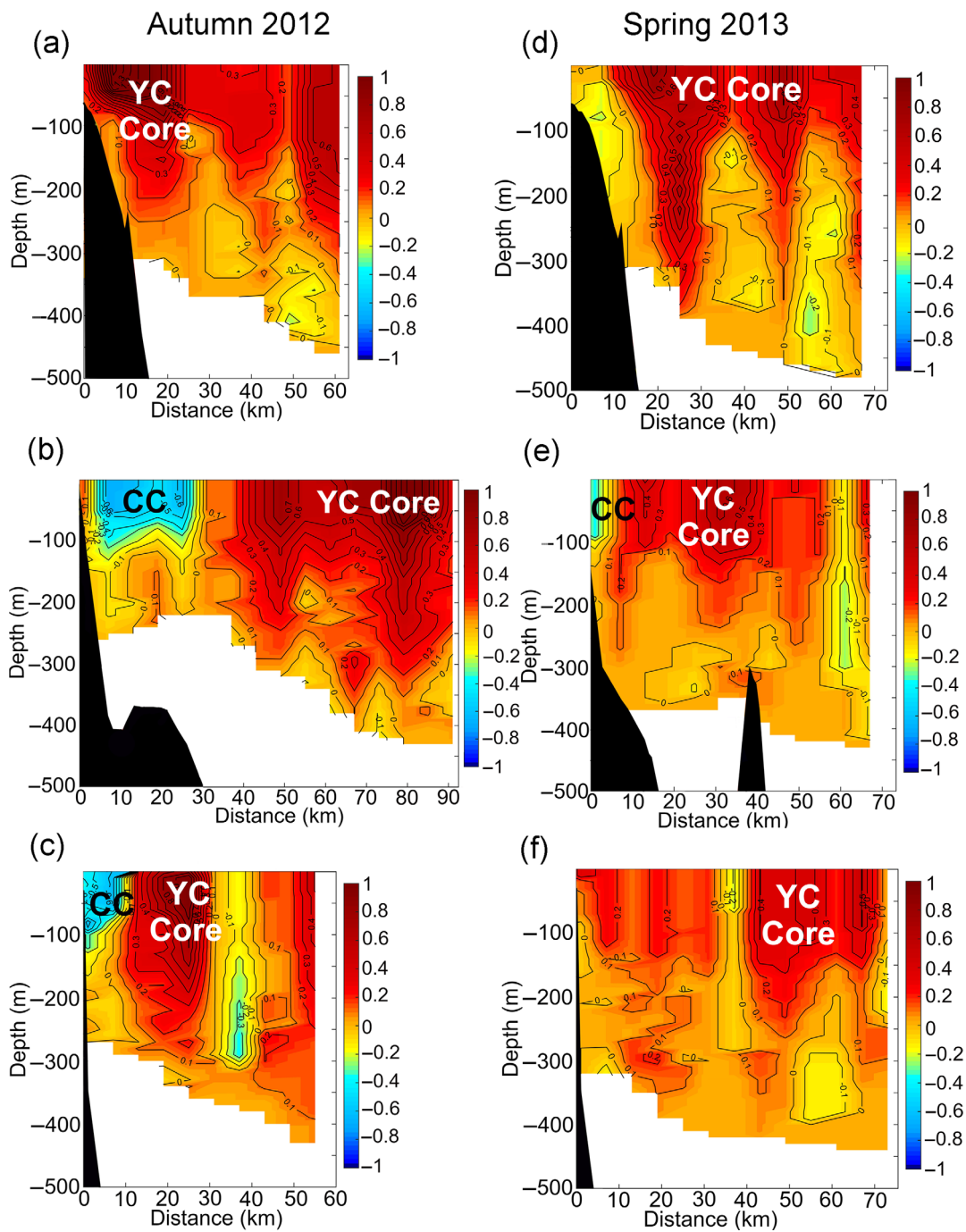


Fig 5. Cross-sectional distribution of geostrophic flow velocity (m s^{-1}) between the surface and 500 m at the northern (a, d), central (b, e), and southern (c, f) sections of the study area during the autumn 2012 cruise (left column) and the spring 2013 cruise (right column). The derived geostrophic velocity is perpendicular to the transect and referred to the isopycnal of 27 kg m^{-3} . YC Core, Yucatan Current Core.

cruise. During the autumn cruise (Fig. 6a–c), there was an anticyclonic eddy to the east of the YC and the velocity of the geostrophic currents off the Yucatan Peninsula increased northward. However, of the four ADCPs, the one moored in the Cozumel channel measured the strongest velocities, at slightly over 1 m s^{-1} , consistent with the YC core being closer

to the coast during the autumn cruise (see Fig. 5a–c). The presence of the countercurrent south of Cozumel obtained with the geostrophic calculations from the CTD survey (see Fig. 5c) is not registered on this altimetry-deduced flow field, mainly because the CC was close to the coast, where altimetry measurements are not reliable. However, the general pattern of

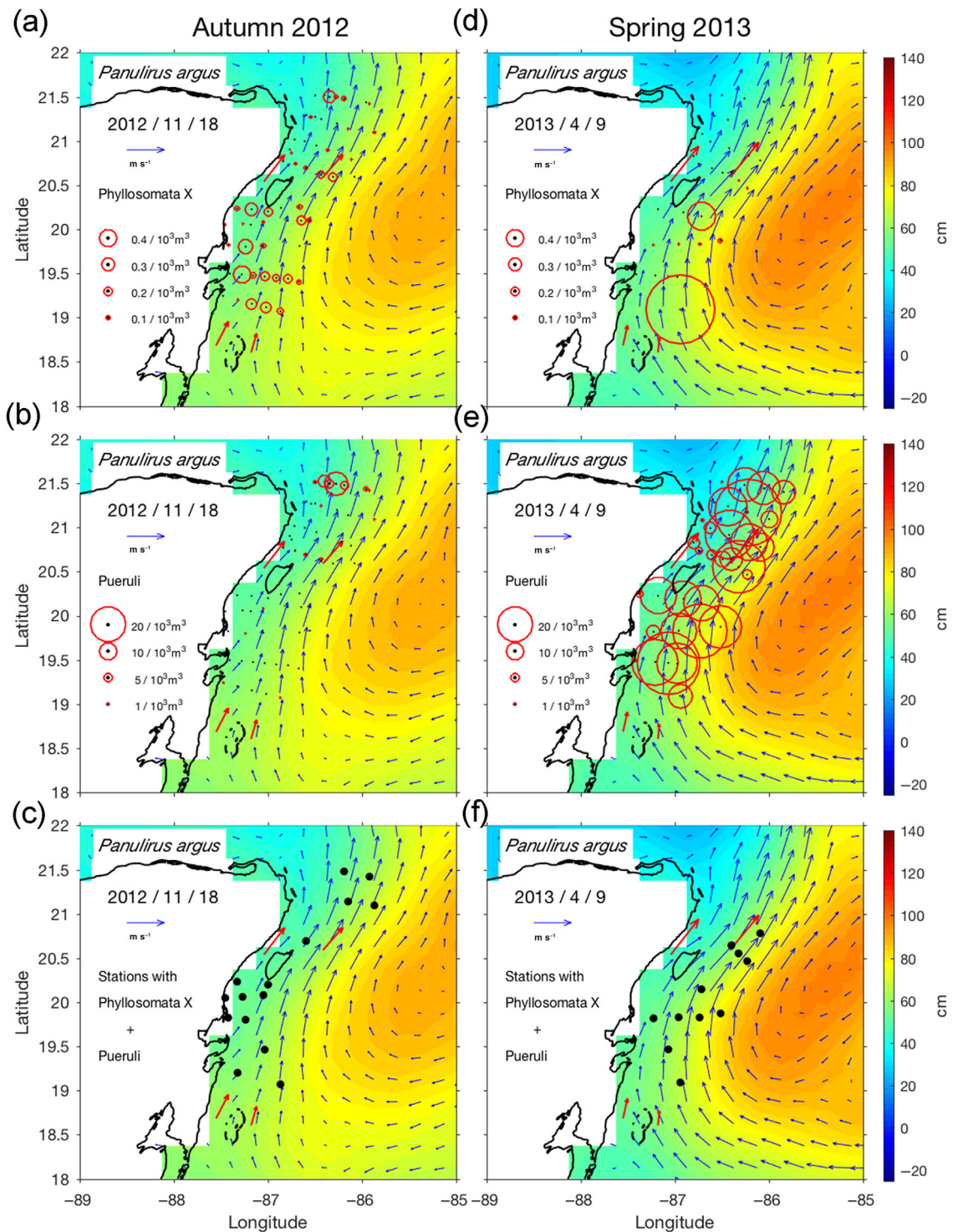


Fig 6. *Panulirus argus*. Distribution and density of (a, d) final stage phyllosomata (stage X) and (b, e) pueruli, and (c, f) stations with co-occurring final phyllosomata and pueruli during the autumn 2012 cruise (left column) and the spring 2013 cruise (right column). Note that, for clarity purposes, the density scales differ between stages. Density symbols are superimposed on the surface current field of each cruise. Red arrows are current velocities measured by the four moored ADCPs.

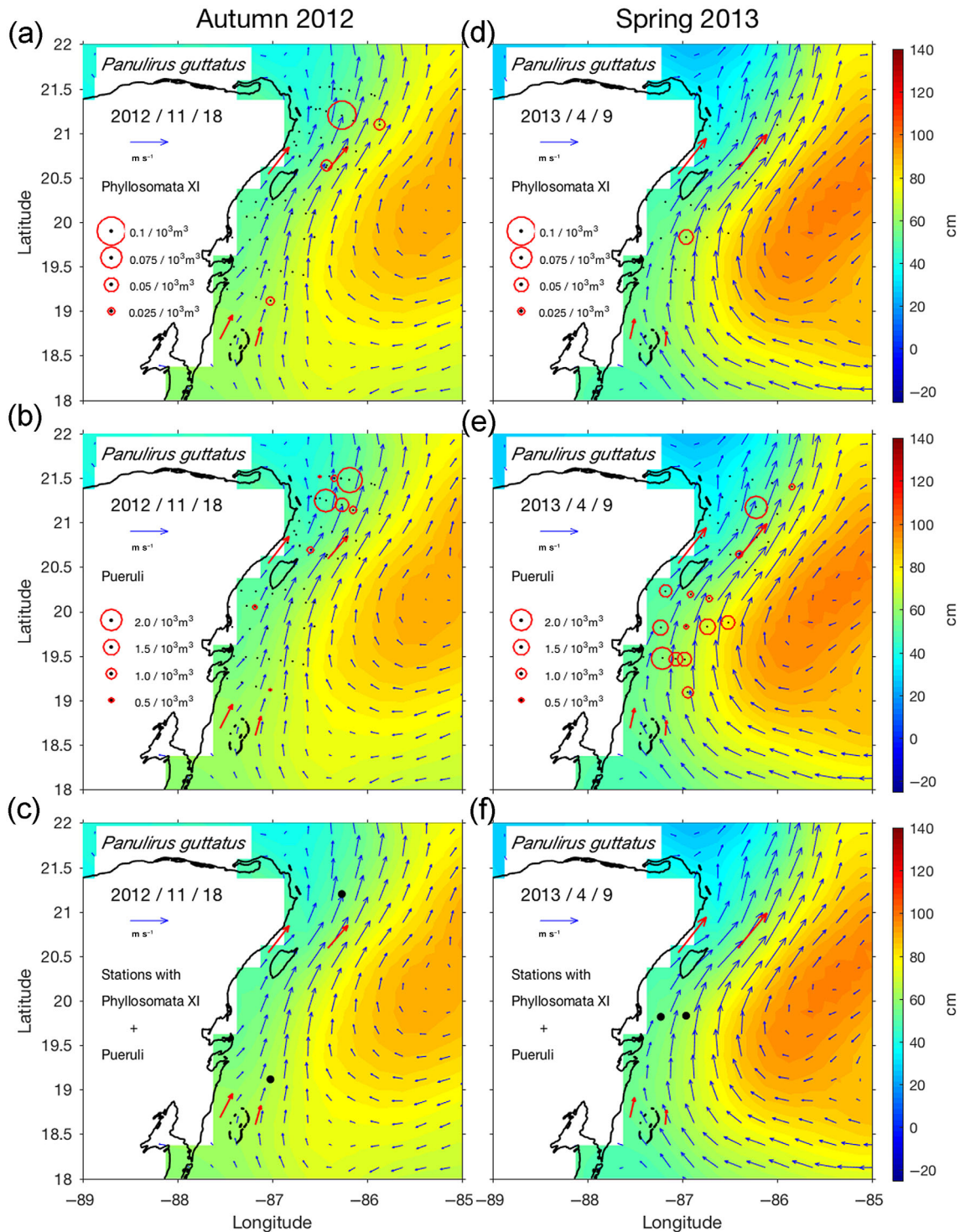


Fig 7. *Panulirus guttatus*. Distribution and density of (a, d) final stage phyllosomata (stage X) and (b, e) pueruli, and (c, f) stations with co-occurring final phyllosomata and pueruli during the autumn 2012 cruise (left column) and the spring 2013 cruise (right column). Note that the density scales differ between stages. Density symbols are superimposed on the surface current field of each cruise. Red arrows are current velocities measured by the four moored ADCPs.

the YC core being separated from the coast south of Cozumel and closer to shore toward the north is consistent in both data sets and direct current observations (red arrows in Fig. 6a–c).

During the spring cruise (Fig. 6d–f), a large anticyclonic/cyclonic eddy system occurred also to the east of our study area, south of Cuba. Differences in sea surface height were

more pronounced during the spring cruise than during the autumn cruise, resulting in stronger geostrophic currents. The ADCP moored off NE Cozumel measured the stronger velocities ($\sim 1.5 \text{ m s}^{-1}$), consistent with the YC core being farther from the coast during the spring cruise than during the autumn cruise.

Density and distribution of final phyllosomata and pueruli

In total, we caught 191 final (gilled) stage phyllosomata and 1170 pueruli in both cruises, mostly belonging to

P. argus (96.3% of all final phyllosomata and 94.9% of all pueruli). Most phyllosomata were caught in the autumn cruise, whereas most pueruli were caught in the spring cruise. Also, virtually all pueruli (95.7% of *P. argus* and 100% of *P. guttatus*) were caught in the neuston net, whereas virtually all phyllosomata (96.7% of *P. argus* and 100% of *P. guttatus*) were caught in the mid-water trawl. Larval and postlarval densities of each lobster species per cruise are visualized superimposed on the current field of each cruise (Figs. 6, 7).

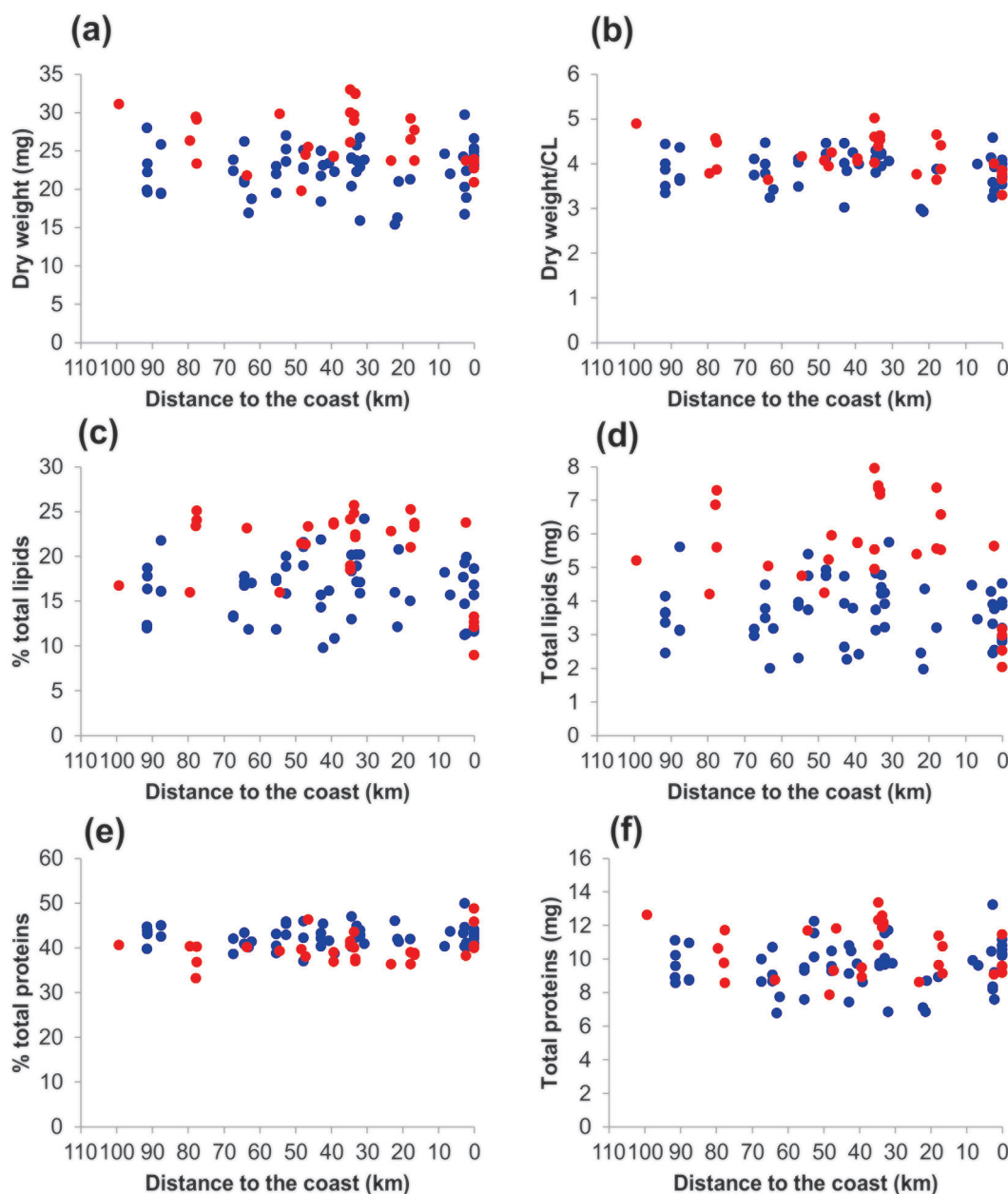


Fig 8. *Panulirus argus*. Comparison of (a) dry weight (mg), (b) condition factor (dry weight/carapace length), (c) percentage of total lipids, (d) total lipid (mg), (e) % total proteins, and (f) total proteins (mg) between pueruli collected in sampling stations along a range of distances to the coast (100 to 0.3 km) in the autumn 2012 cruise (blue dots) and in the spring 2013 cruise (red dots).

Panulirus argus

In the autumn cruise, we collected 123 final phyllosomata (stage X) and 127 pueruli of *P. argus*. Of the 63 sampling stations in this cruise, final phyllosomata were caught in 37 stations (58.7%) throughout the study area, but the highest densities (~0.4 larvae per 1000 m³) were obtained in several stations close to the coast, especially south of Cozumel Island (Fig. 6a). Pueruli of *P. argus* occurred in 28 of the stations (44.4%), usually at greater densities than phyllosomata, but the highest densities of pueruli (between 2 and 13 postlarvae per 1000 m³) were obtained in stations located in the Yucatan Channel area (Fig. 6b). Both final phyllosomata and pueruli of *P. argus* co-occurred in 15 of the 63 sampling stations (23.8%) (Fig. 6c). Most of these stations were located very close to the coast in an area south of Cozumel and off Bahía de la Ascensión (~20°N), but a few were located farther from the coast in the Yucatan Channel area.

In the spring cruise, we caught 61 final phyllosomata and 982 pueruli of *P. argus*. Final phyllosomata appeared in 14 of the 34 sampling stations in this cruise (41.2%), with most individuals concentrated in two offshore stations to the east and south of Cozumel at densities of 0.6 and 1.6 larvae per 1000 m³, respectively (Fig. 6d). Pueruli were so abundant in this cruise that they occurred in 33 of the 34 stations (97%) at densities ranging from 0.5 to 37.8 postlarvae per 1000 m³, with the highest densities in stations relatively far from the coast (Fig. 6e). Final phyllosomata and pueruli were caught together in 11 of the 34 stations (32.3%), located farther from the coast than in the autumn cruise (Fig. 6f).

Panulirus guttatus

For *P. guttatus*, catches of final phyllosomata and pueruli were far lower than for *P. argus*. Prior to our study, the final stage of *P. guttatus* had not been captured and remained undescribed. Because the *P. guttatus* larvae were staged based on Baisre and Alfonso (1994), we refer to the final stage as the phyllosoma XI. In the autumn cruise, we caught five final-stage phyllosomata in four of the 63 sampling stations (6.3%); therefore, the densities were quite low (≤ 0.1 larvae per 1000 m³) (Fig. 7a). Twenty-two pueruli of *P. guttatus* occurred in nine stations (14.3%), with most of the catch (1.3–2.4 postlarvae per 1000 m³) concentrated in three stations close to the Yucatan channel (Fig. 7b). Only two stations yielded both final phyllosomata and pueruli of *P. guttatus* (Fig. 7c). In the spring cruise, two final phyllosomata of *P. guttatus* were caught in two of the 34 stations (5.9%) at very low densities (≤ 0.05 larvae per 1000 m³) (Fig. 7d), whereas 38 pueruli were present in 14 stations (41.2%) located mostly south of Cozumel, at densities ranging from 0.5 to 2.1 postlarvae per 1000 m³ (Fig. 7e). Only two stations with final phyllosomata also yielded pueruli (Fig. 7f).

Size distribution of pueruli

The size range of pueruli of both species was broad (*P. argus*: 4.33–7.55 mm CL; *P. guttatus*: 7.52–11.0 mm CL). In

Table 1. *Panulirus argus*. Comparison of mean dry weight, total lipid (mg), total protein (mg), total lipid and protein as a percentage of dry weight, and a condition factor (dry weight/carapace length) in pueruli collected in the autumn 2012 and the spring 2013 cruise. Numbers in parentheses are standard deviations. *p* values are derived from separate ANCOVAs comparing each variable between cruises and along distances to the shore (0.3–100 km). The effect of distance to the shore was not significant (*p* values: 0.174–0.924).

| | Autumn 2012 | Spring 2013 | <i>p</i> value |
|--------------------|--------------|--------------|----------------|
| Dry weight (mg) | 22.46 (3.06) | 26.46 (3.66) | <0.0001 |
| Total lipid (mg) | 3.69 (0.91) | 5.53 (1.54) | <0.0001 |
| % Total lipid | 16.42 (3.35) | 20.72 (4.55) | <0.0001 |
| Total protein (mg) | 9.54 (1.36) | 10.49 (1.53) | 0.0039 |
| % Total protein | 42.49 (2.32) | 39.74 (3.21) | <0.0001 |
| Dry weight/CL | 3.88 (0.40) | 4.15 (0.42) | 0.0056 |
| <i>N</i> | 58 | 29 | |

P. argus, size of pueruli differed significantly between cruises ($F_{1,1093} = 52.019$, $p < 0.0001$), with a smaller value in autumn (mean \pm SD: 5.62 \pm 0.35 mm CL, $n = 114$) than in spring (6.01 \pm 0.56 mm CL, $n = 981$). The size of pueruli of *P. guttatus* varied significantly with cruise as well ($F_{1,56} = 79.495$, $p < 0.0001$), also showing a smaller value in autumn (mean \pm SD: 8.34 \pm 0.48 mm CL, $n = 20$) than in spring (9.68 \pm 0.57 mm CL, $n = 38$).

Energy reserves of pueruli of *P. argus*

No trend was evident for any of the six biochemical variables measured for pueruli of *P. argus* across the range of distances to the coast of sampling stations in either cruise (Fig. 8). This was confirmed by results of ANCOVAs, which revealed no significant effect of distance to the coast for any of the six variables (range in *p* values: 0.174–0.924). However, all six variables differed significantly between cruises. Interestingly, except for percent TP, the mean value of all variables was significantly higher for pueruli collected in the spring cruise (Table 1).

Discussion

This is the first study addressing the question of where metamorphosis of *P. argus* and *P. guttatus* occurs, and the first to obtain the final, still undescribed phyllosoma stage of *P. guttatus*. We found an important presence of final stage phyllosomata and pueruli of *P. argus* and, to a lesser extent, of *P. guttatus*, in oceanic waters along the Mexican Caribbean up to ~100 km from the shore (the maximum distance to the shore of our transects), but our results confirmed that metamorphosis of both species occurs mainly associated with the YC core.

Our sampling design was based on the interannual seasonal pattern of postlarval settlement of *P. argus*, which shows a major peak in autumn and a minor peak in spring (Briones-Fourzán et al. 2008); therefore, we expected to obtain more final larvae and postlarvae of *P. argus* in the autumn 2012 cruise than in the spring 2013 cruise. Most final phyllosomata were indeed caught in the former, but far more pueruli were caught in the latter. To our knowledge, the 982 pueruli of *P. argus* caught in our spring cruise is the largest number of pueruli of any spiny lobster species caught in any one cruise. The majority of pueruli were caught in the neuston net, underlining their tendency to swim in the first few centimeters of the water column in dark nights (Phillips and Olsen 1975; Calinski and Lyons 1983). Therefore, our results may simply reflect the differing moonlight intensity between both cruises, with more brightly moonlit nights in the autumn cruise (conducted between the dates of new moon and full moon) and more dark nights in the spring cruise (conducted between the dates of the last and first lunar quarters). Indeed, the mid-water trawl caught 26% of the 127 pueruli of *P. argus* obtained in the autumn cruise, but only 4% of the 982 obtained in the spring cruise.

In other species, most pueruli have also been caught within the first meter of the water column in dark nights (*P. cygnus*: Phillips et al. 1978; *Panulirus ornatus* and *Panulirus penicillatus*: Dennis et al. 2001), but at greater depths in nights with higher illuminance (Phillips et al. 1978; Pearce et al. 1992). Also, rough sea conditions, which further appear to favor the concentration of pueruli in surface waters (Ritz 1972; Phillips et al. 1978), prevailed in both of our cruises, but particularly in the spring cruise. In contrast with *P. argus*, all pueruli of *P. guttatus* were caught in the neuston net. Whether this occurrence reflects a difference in behavior between pueruli of *P. argus* and *P. guttatus* or the large difference in the catches of pueruli of both species is unknown.

Unlike pueruli, most final phyllosomata were caught in the mid-water trawl. Only 2 of the 123 final phyllosomata of *P. argus* from the autumn cruise (1.6%) and 4 of the 63 from the spring cruise (6.4%), but none of the final phyllosomata of *P. guttatus*, were caught in the neuston net. These results suggest that, even in dark nights, phyllosomata are more dispersed in the water column than pueruli are. Although vertical migrations of phyllosomata, which descend in the water column during the day and ascend at night, potentially modulate their advection (Rimmer and Phillips 1979; Bradford et al. 2005), their eye structure suggests that they spend most of their planktonic life in reasonably well-illuminated regions of the ocean (Mishra et al. 2006). There is no information on how deep the vertical migrations of *P. guttatus* can go, but in the case of *P. argus*, few phyllosomata have been found at depths > 100 m, even during the day (Alfonso et al. 1999; Butler et al. 2011), and late stages have been caught mainly in the first 25 m of the water column in dark nights (Austin 1972; Alfonso et al. 1995; Canto-García et al. 2016). Also, phyllosomata of

P. argus do not appear to go below the 24°C isotherm (Yeung and McGowan 1991; Alfonso et al. 1999), which in our cruises was generally well above the 100 m isobath. Therefore, for those phyllosomata that are entrained by the swift YC, which is coherent within at least the upper 130 m of the water column (Cetina et al. 2006; the present study), vertical migration is unlikely to modulate their advection.

The superposition of the sampling stations with co-occurring final phyllosomata and pueruli on the current fields supports our hypothesis that metamorphosis occurs within the YC and is mainly associated with the YC core. In the autumn 2012 cruise, these stations were mostly located south of Cozumel Island and closer to the shore, whereas in the spring 2013 cruise they were mostly located farther from the shore. It is important to underline that the location of the YC core does not follow a fixed seasonal pattern but is rather related with temporal shifts in the latitude of impingement of the Cayman current on the eastern coast of the Yucatan Peninsula, which depends on the size and intensity of mesoscale eddies (both cyclonic and anticyclonic) flowing with the current (Cetina et al. 2006; Carrillo et al. 2015). During both our cruises, interesting circulation features included the CC in the central-southern sections of our study area, which had been inferred by Merino (1986) from information provided by drift cards, and the presence of a cyclonic eddy south of Cozumel Island. This eddy appears to be a persistent feature since it was also observed in June 2000 during a shipboard ADCP survey of the region (Chávez et al. 2003), and during two oceanographic cruises conducted in March 2006 and January 2007 (Carrillo et al. 2015). The coastal eddy and the CC may aid in the local retention of phyllosomata and the shoreward migration of pueruli (Yeung et al. 2001), as suggested by the location over these features of several sampling stations with both final phyllosomata and pueruli of *P. argus* in the autumn cruise, and with many pueruli in the spring cruise.

Relative to the autumn cruise, pueruli of both species were larger in the spring cruise, and those of *P. argus* were also in a better nutritional condition, as suggested by their higher values of DW, condition index, and TL content. The size and condition of pueruli are known to vary temporally (Yeung et al. 2001; Martínez-Calderón et al. 2018), possibly related to variation in the water temperature throughout the larval development (Matsuda and Yamakawa 1997). Espinosa-Magaña et al. (2018) compared the TL content between a subsample of the final phyllosomata and nektonic pueruli of *P. argus* collected in our cruises, and the ensuing benthic stages (transparent benthic pueruli, pigmented pueruli, and first juveniles), collected in the shore during the same seasons. They found that the greatest decline in TL occurred between final phyllosomata and nektonic pueruli in autumn, when surface temperatures were significantly higher than in spring, suggesting a greater energy cost of metamorphosis at warmer temperatures, but between nektonic and benthic pueruli in spring, when the YC was stronger, potentially increasing the

energy cost of shoreward swimming (Espinosa-Magaña et al. 2018). Differences in size and condition could also reflect variations in the quality and quantity of food. Phyllosomata are omnivorous but prefer gelatinous zooplankton (O'Rorke et al. 2015 and references therein), which tends to be more abundant offshore near shelf breaks (Luo et al. 2014; Greer et al. 2020). Gelatinous zooplankton can accumulate dispersed microbial nutrients and make them available as larger prey for late stage phyllosomata, as suggested by analyses of fatty acids (Wang et al. 2014; Briones-Fourzán et al. 2019). A better nutritional condition could influence the subsequent settlement of pueruli (Wang et al. 2014), but whether survival rates differ between large and small pueruli of a given species has not been determined.

Irrespective of their size at metamorphosis, the nonfeeding pueruli must use the lipid reserves accumulated as phyllosomata to swim toward the shore (Wilkin and Jeffs 2011). A depletion of the energy stores used to fuel the shoreward migration has been found in pueruli captured inshore compared to those captured offshore in *J. edwardsii* in New Zealand (Jeffs et al. 1999, 2001) and *P. cygnus* in Australia (Phillips et al. 2006b; Limbourn et al. 2009). We hypothesized that this would also happen in *P. argus* but, contrary to our expectations, none of the biochemical variables considered for pueruli of *P. argus* declined during the shoreward migration in either cruise. Briones-Fourzán et al. (2019) also did not find significant differences in the fatty acid profiles between nektonic pueruli of *P. argus* from our autumn 2012 cruise and recently settled pueruli obtained in coastal collectors. Together, these results suggest that, although metamorphosis can occur over the entire range of distances to the shore spanned by our sampling stations, only those pueruli metamorphosing within a portion of that range may make it to the Mexican Caribbean coast.

Swimming distances and the potential success of the shoreward migration by pueruli are greatly influenced by oceanic forces (Phillips et al. 2006b; Limbourn et al. 2009); therefore, it has been proposed that metamorphosis must occur offshore but close to the shelf break for the pueruli to be able to reach the shore, which would be unlikely if metamorphosis occurs much further offshore (Phillips and McWilliam 2009). In the permanently strong YC (1 m s^{-1} on average), an embedded particle could be advected 200 km in only 55.5 h; consequently, the passage of these larvae through the region would be expected to be relatively short ($\sim 2 \text{ d}$). However, based on data from drift cards released along the Mexican Caribbean, Merino (1986) concluded that although particles in superficial waters at distances $\geq 15 \text{ km}$ from the coast would indeed drift along with the swift YC, those at distances $\leq 10 \text{ km}$ would tend to drift toward the coast. Moreover, pueruli are not merely drifting particles, but strong swimmers able to swim into or along ocean currents (Phillips and Olsen 1975; Kough et al. 2014). Pueruli of *J. edwardsii* experimentally swum in a kreisel for 2, 3, or 5 d, alternated between extended periods of

swimming at the speed of the current and drifting with the water flow. Interestingly, the TL of pueruli swum for 2 d did not differ significantly from that of a control group, whereas the TL of pueruli swum for 3 and 5 d was significantly lower (García-Echauri and Jeffs 2018).

Pueruli of *P. argus* swimming in circular floating arenas deployed in the sea off the Florida coast (U.S.A.) were observed to swim directionally day and night. They swam with the current, which ran parallel to the coast (as the YC does), but oriented relative to the tide flow and the wind in such a way as to place them on a shoreward trajectory (Kough et al. 2014). This orientation ability, while swimming at a speed of $7\text{--}10 \text{ cm s}^{-1}$ (as measured by Calinski and Lyons 1983), could allow pueruli of *P. argus* metamorphosing within $\sim 12 \text{ km}$ from the eastern Yucatan coast to reach the settlement habitats in a few hours to less than 2 d without a significant loss of energy reserves (García-Echauri and Jeffs 2018), as found in our study. Even some pueruli metamorphosing farther than 12 km from the coast may be helped in their shoreward migration if encountering favorable flow features, such as the persistent coastal eddy south of Cozumel, which extends to around 20 km from the coast (Carrillo et al. 2015), as well as the CC in the central and southern sections of our study area, which extended to 30 km from the coast in our autumn cruise. The onshore transport of pueruli can be further enhanced by the dominant trade winds, which blow toward the coast, and by large waves generated by extreme weather events (Caputi and Brown 1993; Briones-Fourzán et al. 2008). In contrast, pueruli metamorphosing farther away than 30 km from this coast or closer to the Yucatan Channel are more likely to be carried by the swift YC into the Gulf of Mexico, riding on the Loop Current, and potentially settle elsewhere, for example, along the Florida Keys or the Cuban coast (Merino 1986; Lara-Hernández et al. 2019; Segura-García et al. 2019). Others might enter the eddy system east of the YC, eventually reaching the southern coast of Cuba or recirculating within the eddies (Martín et al. 2017), and others would undoubtedly be lost due to exhausted energetic reserves and a declining swimming response with increasing pueruli age (Wilkin and Jeffs 2011; Fitzgibbon et al. 2014).

Building upon earlier studies on different spiny lobster species, our study increased insight into the oceanic zones where metamorphosis of spiny lobsters may occur. Our results suggest that metamorphosing within strong boundary currents, which by definition are determined by the presence of a coastline, may increase the chances of pueruli arriving more quickly to a shore. However, settlement of pueruli in the coastal habitats is known to vary broadly in time (reviewed in Phillips et al. 2006a). In the case of the Mexican Caribbean coast, our results further suggest that the intra- and inter-annual variation in settlement of *P. argus* postlarvae (Briones-Fourzán et al. 2008) may be partially underlain by the variability in the velocity and location of the YC core, the associated CC, and the coastal eddy.

References

- Alfonso, I., M. P. Frías, J. Baisre, and B. Hernández. 1995. Distribución vertical de filosomas de *Panulirus argus* y su relación con algunos factores hidroclimáticos al S del Golfo de Batabanó, Cuba. *Rev. Cubana Inv. Pesq.* **19**: 3–9.
- Alfonso, I., M. P. Frías, and J. Baisre. 1999. Distribución, abundancia y migración vertical de la fase larval de la langosta comercial *Panulirus argus* en aguas cubanas. *Rev. Inv. Mar.* **20**: 23–32.
- Austin, H. M. 1972. Notes on the distribution of phyllosoma of the spiny lobster *Panulirus* spp., in the Gulf of Mexico. *Proc. Natn. Shellfish Assoc.* **62**: 26–30.
- Baisre, J. A., and I. Alfonso. 1994. Later stage larvae of *Panulirus guttatus* (Latreille, 1804) (Decapoda, Palinuridae) with notes on the identification of phyllosomata of *Panulirus* in the Caribbean Sea. *Crustaceana* **66**: 32–44. doi:10.1163/156854094X00134
- Bligh, E. G., and W. J. Dyer. 1959. A rapid method of total lipid extraction and purification. *Can. J. Biochem. Physiol.* **37**: 911–917. doi:10.1139/o59-099
- Bradford, R. W., B. D. Bruce, S. M. Chiswell, J. D. Booth, A. Jeffs, and S. Wotherspoon. 2005. Vertical distribution and diurnal migration patterns of *Jasus edwardsii* phyllosomas off the east coast of the North Island, New Zealand. *N. Z. J. Mar. Freshw. Res.* **39**: 593–604. doi:10.1080/00288330.2005.9517338
- Briones-Fourzán, P. 1994. Variability in postlarval recruitment of the spiny lobster *Panulirus argus* (Latreille, 1804) to the Mexican Caribbean coast. *Crustaceana* **66**: 326–340. doi:10.1163/156854094X00062
- Briones-Fourzán, P., and P. S. McWilliam. 1997. Puerulus of the spiny lobster *Panulirus guttatus* (Latreille, 1804) (Palinuridae). *Mar. Freshw. Res.* **48**: 699–706. doi:10.1071/MF97130
- Briones-Fourzán, P., J. Candela, and E. Lozano-Álvarez. 2008. Postlarval settlement of the spiny lobster *Panulirus argus* along the Mexican Caribbean coast: Patterns, influence of physical factors, and possible sources of origin. *Limnol. Oceanogr.* **53**: 970–985. doi:10.4319/lo.2008.53.3.0970
- Briones-Fourzán, P., and E. Lozano-Álvarez. 2013. Essential habitats for *Panulirus* spiny lobsters, p. 186–220. *In* B. F. Phillips [ed.], *Lobsters: Biology, management, aquaculture and fisheries*, 2nd ed. Wiley-Blackwell.
- Briones-Fourzán, P., E. Magallón-Gayón, and E. Lozano-Álvarez. 2013. Increased reproductive opportunity: A potential benefit of seasonal aggregation for a little-gregarious and highly sedentary spiny lobster. *Mar. Biol. Res.* **9**: 77–87. doi:10.1080/17451000.2012.727431
- Briones-Fourzán, P., A. F. Espinosa-Magaña, E. Lozano-Álvarez, and A. Jeffs. 2019. Analysis of fatty acids to examine larval and settlement biology of the Caribbean spiny lobster *Panulirus argus*. *Mar. Ecol. Prog. Ser.* **630**: 137–148. doi:10.3354/meps13127
- Butler, M. J., IV, C. B. Paris, J. S. Goldstein, H. Matsuda, and R. K. Cowen. 2011. Behavior constrains the dispersal of long-lived spiny lobster larvae. *Mar. Ecol. Prog. Ser.* **422**: 223–237. doi:10.3354/meps08878
- Calinski, M. D., and W. G. Lyons. 1983. Swimming behavior of the puerulus of the spiny lobster *Panulirus argus* (Latreille, 1804) (Crustacea: Palinuridae). *J. Crustac. Biol.* **3**: 329–335. doi:10.2307/1548136
- Candela, J., S. Tanahara, M. Crepon, B. Barnier, and J. Sheinbaum. 2003. Yucatan Channel flow: Observations versus CLIPPER ATL6 and MERCATOR PAM models. *J. Geophys. Res.* **108**: C123385. doi:10.1029/2003JC001961
- Canto-García, A., J. Goldstein, E. Sosa-Cordero, and L. Carrillo. 2016. Distribution and abundance of *Panulirus* spp. phyllosomas off the Mexican Caribbean coast. *Bull. Mar. Sci.* **92**: 207–227. doi:10.5343/bms.2015.1015
- Caputi, N., and R. S. Brown. 1993. The effect of environment on puerulus settlement of the western rock lobster (*Panulirus cygnus*) in Western Australia. *Fish. Oceanogr.* **2**: 1–10. doi:10.1111/j.1365-2419.1993.tb00007.x
- Carrillo, L., J. L. Largier, E. Johns, R. Smith, and J. Lamkin. 2015. Pathways and upper hydrography in the Mesoamerican Barrier Reef System-part 1: Circulation. *Cont. Shelf Res.* **109**: 164–176. doi:10.1016/j.csr.2015.09.014
- Carrillo, L., E. M. Johns, R. H. Smith, J. T. Lamkin, and J. L. Largier. 2016. Pathways and hydrography in the Mesoamerican Barrier Reef System-part 2: Water masses and thermal structure. *Cont. Shelf Res.* **120**: 41–58. doi:10.1016/j.csr.2016.03.014
- Cetina, P., J. Candela, J. Sheinbaum, J. Ochoa, and A. Badam. 2006. Circulation along the Mexican Caribbean coast. *J. Geophys. Res.* **111**: C08021. doi:10.1029/2005JC003056
- Chávez, G., J. Candela, and J. Ochoa. 2003. Subinertial flows and transports in Cozumel Channel. *J. Geophys. Res.* **108**: 3037. doi:10.1029/2002JC001456
- Chiswell, S. M., and J. D. Booth. 2005. Distribution of mid- and late-stage *Jasus edwardsii* phyllosomas: Implications for larval recruitment processes. *N. Z. J. Mar. Freshw. Res.* **39**: 1157–1170. doi:10.1080/00288330.2005.9517382
- Dennis, D. M., C. R. Pitcher, and T. D. Skewes. 2001. Distribution and transport pathways of *Panulirus ornatus* (Fabricius, 1776) and *Panulirus* spp. larvae in the Coral Sea, Australia. *Mar. Freshw. Res.* **52**: 1175–1185. doi:10.1071/MF01186
- Espinosa-Magaña, A. F., P. Briones-Fourzán, A. Jeffs, and E. Lozano-Álvarez. 2018. Energy cost of the onshore transport of postlarvae of the Caribbean spiny lobster. *Bull. Mar. Sci.* **94**: 801–819. doi:10.5343/bms.2017.1145
- Fitzgibbon, Q. P., A. G. Jeffs, and S. C. Battaglione. 2014. The Achilles heel for spiny lobsters: The energetics of the non-feeding post-larval stage. *Fish. Fish.* **15**: 312–326. doi:10.1111/faf.12018
- Folch, J., M. Lees, and G. H. Sloane-Stanley. 1957. A simple method for the isolation and purification of total lipids

- from animal tissues. *J. Biol. Chem.* **226**: 497–509. doi:[10.1016/S0021-9258\(18\)64849-5](https://doi.org/10.1016/S0021-9258(18)64849-5)
- García-Echauri, L. L., and A. Jeffs. 2018. Swimming energetics of the post-larvae of the spiny lobster *Jasus edwardsii* in New Zealand. *Bull. Mar. Sci.* **94**: 821–834. doi:[10.5343/bms.2017.1116](https://doi.org/10.5343/bms.2017.1116)
- Goldstein, J. S., H. Matsuda, T. Takenouchi, and M. J. Butler IV. 2008. The complete development of larval Caribbean spiny lobster *Panulirus argus* (Latreille, 1804) in culture. *J. Crustac. Biol.* **28**: 306–327. doi:[10.1163/20021975-99990376](https://doi.org/10.1163/20021975-99990376)
- Goldstein, J. S., H. Matsuda, T. R. Matthews, A. Fumihiko, and T. Yamakawa. 2019. Development in culture of larval spotted spiny lobster *Panulirus guttatus* (Latreille, 1804) (Decapoda: Achelata: Palinuridae). *J. Crustac. Biol.* **39**: 574–581. doi:[10.1093/jcbiol/ruz055](https://doi.org/10.1093/jcbiol/ruz055)
- Greer, A. T., and others. 2020. High-resolution sampling of a broad marine life size spectrum reveals differing size-and composition-based associations with physical oceanographic structure. *Front. Mar. Sci.* **7**: 542701. doi:[10.3389/fmars.2020.542701](https://doi.org/10.3389/fmars.2020.542701)
- Griffin, D. A., J. L. Wilkin, C. F. Chubb, A. Pearce, and N. Caputi. 2001. Ocean currents and the larval phase of Australian western rock lobster, *Panulirus cygnus*. *Mar. Freshw. Res.* **52**: 1187–1199. doi:[10.1071/MF01181](https://doi.org/10.1071/MF01181)
- Inoue, N., and H. Sekiguchi. 2009. Can long-term variation in catch of Japanese spiny lobster *Panulirus japonicus* be explained by larval supply through the Kuroshio Current? *N. Z. J. Mar. Freshw. Res.* **43**: 89–99. doi:[10.1080/00288330909509984](https://doi.org/10.1080/00288330909509984)
- Jeffs, A. G., M. E. Wilmott, and R. M. G. Wells. 1999. The use of energy stores in the puerulus of the spiny lobster *Jasus edwardsii* across the continental shelf of New Zealand. *Comp. Biochem. Physiol. A Mol. Integr. Physiol.* **123**: 351–357. doi:[10.1016/S1095-6433\(99\)00073-2](https://doi.org/10.1016/S1095-6433(99)00073-2)
- Jeffs, A. G., S. M. Chiswell, and J. D. Booth. 2001. Distribution and condition of pueruli of the spiny lobster *Jasus edwardsii* offshore from north-east New Zealand. *Mar. Freshw. Res.* **52**: 1211–1216. doi:[10.1071/MF01182](https://doi.org/10.1071/MF01182)
- Jeffs, A. G., J. C. Montgomery, and C. T. Tindle. 2005. How do spiny lobster post-larvae find the coast? *N. Z. J. Mar. Freshw. Res.* **39**: 605–617. doi:[10.1080/00288330.2005.9517339](https://doi.org/10.1080/00288330.2005.9517339)
- Kough, A. S., C. B. Paris, and E. Staaterman. 2014. In situ swimming and orientation behavior of spiny lobster (*Panulirus argus*) postlarvae. *Mar. Ecol. Prog. Ser.* **504**: 207–219. doi:[10.3354/meps10748](https://doi.org/10.3354/meps10748)
- Lara-Hernández, J. A., J. Zavala-Hidalgo, L. Sanvicente-Añorve, and P. Briones-Fourzán. 2019. Connectivity and larval dispersal pathways of *Panulirus argus* in the Gulf of Mexico: A numerical study. *J. Sea Res.* **155**: 101814. doi:[10.1016/j.seares.2019.101814](https://doi.org/10.1016/j.seares.2019.101814)
- Lemmens, J. W. T. J. 1994. Biochemical evidence for absence of feeding in pueruli larvae of the western rock lobster *Panulirus cygnus* (Decapoda: Palinuridae). *Mar. Biol.* **118**: 383–391. doi:[10.1007/BF00350295](https://doi.org/10.1007/BF00350295)
- Limbourn, A. J., R. C. Babcock, D. J. Johnston, P. D. Nichols, and E. B. Knott. 2009. Spatial and temporal variation in lipid and fatty acid profiles of western rock lobster pueruli at first settlement: Biochemical indicators of diet and nutritional status. *Mar. Freshw. Res.* **60**: 810–823. doi:[10.1071/MF08244](https://doi.org/10.1071/MF08244)
- Lozano-Álvarez, E., P. Briones-Fourzán, J. P. Huchin-Mian, I. Segura-García, J. P. Ek-Huchim, M. Améndola-Pimenta, and R. Rodríguez-Canul. 2015. *Panulirus argus* virus 1 detected in oceanic postlarvae of Caribbean spiny lobster: Implications for disease dispersal. *Dis. Aquat. Organ.* **117**: 165–170. doi:[10.3354/dao02935](https://doi.org/10.3354/dao02935)
- Luo, J. Y., B. Grassian, D. Tang, J.-O. Irisson, A. T. Greer, C. M. Guigand, S. McClatchie, and R. K. Cowen. 2014. Environmental drivers of the fine-scale distribution of a gelatinous zooplankton community across a mesoscale front. *Mar. Ecol. Prog. Ser.* **510**: 129–149. doi:[10.3354/meps10908](https://doi.org/10.3354/meps10908)
- Manzanilla-Domínguez, H., and R. Gasca. 2004. Distribution and abundance of phyllosoma larvae (Decapoda: Palinuridae) in the southern Gulf of Mexico and the western Caribbean Sea. *Crustaceana* **77**: 75–93. doi:[10.1163/156854004323037900](https://doi.org/10.1163/156854004323037900)
- Martín, H., A. Betanzos-Vega, J. Simanca, R. Puga, F. Vijebo, J. Albertsen, and A. Tripp-Quezada. 2017. Simulación de la deriva de larvas de langosta en aguas oceánicas adyacentes a la plataforma suroccidental de Cuba: Aplicación del modelo biofísico LADIM. *Rev. Biol. Mar. Oceanogr.* **52**: 289–297. doi:[10.4067/S0718-19572017000200008](https://doi.org/10.4067/S0718-19572017000200008)
- Martínez-Calderón, R., E. Lozano-Álvarez, and P. Briones-Fourzán. 2018. Morphometric relationships and seasonal variation in size, weight, and a condition index of post-settlement stages of the Caribbean spiny lobster. *PeerJ* **6**: e5297. doi:[10.7717/peerj.5297](https://doi.org/10.7717/peerj.5297)
- Matsuda, H., and T. Yamakawa. 1997. Effects of temperature on growth of the Japanese spiny lobster, *Panulirus japonicus* phyllosomas under laboratory conditions. *Mar. Freshw. Res.* **48**: 791–796. doi:[10.1071/MF97148](https://doi.org/10.1071/MF97148)
- McWilliam, P. S., and B. F. Phillips. 1997. Metamorphosis of the final phyllosoma and secondary lecithotrophy in the puerulus of *Panulirus cygnus* George: A review. *Mar. Freshw. Res.* **48**: 783–790. doi:[10.1071/MF97159](https://doi.org/10.1071/MF97159)
- Merino, M. 1986. Aspectos de la circulación costera superficial del Caribe mexicano con base en observaciones utilizando tarjetas de deriva. *An. Inst. Cienc. del Mar y Limnol. Univ. Nal. Autón. México* **13**: 31–46.
- Mishra, M., A. Jeffs, and V. B. Meyer-Rochow. 2006. Eye structure of the phyllosoma larva of the rock lobster *Jasus edwardsii* (Hutton, 1875): How does it differ from that of the adult? *Invertebr. Reprod. Dev.* **49**: 213–222. doi:[10.1080/07924259.2006.9652209](https://doi.org/10.1080/07924259.2006.9652209)

- Murakami, K., T. Jinbo, and K. Hamasaki. 2007. Aspects of the technology of phyllosoma rearing and metamorphosis from phyllosoma to puerulus in the Japanese spiny lobster *Panulirus japonicus* reared in the laboratory. *Bull. Fish. Res. Agen.* **20**: 59–67.
- O'Rorke, R., S. D. Lavery, M. Wang, R. Gallego, A. M. Waite, L. E. Beckley, P. A. Thompson, and A. G. Jeffs. 2015. Phyllosomata associated with large gelatinous zooplankton: Hitching rides and stealing bites. *ICES J. Mar. Sci.* **72**: i124–i127. doi:10.1093/icesjms/fsu163
- Padilla-Ramos, S., and P. Briones-Fourzán. 1997. Características biológicas de la captura de langosta (*Panulirus* spp.) en Puerto Morelos, Q.R., México. *Cienc. Mar.* **23**: 175–193. doi:10.7773/cm.v23i2.798
- Pearce, A. F., B. F. Phillips, and C. J. Crossland. 1992. Larval distributions across the Leeuwin Current: Report on RV Franklin cruise Fr8/87 in August/September 1987, p. 1–13. CSIRO Mar Labs Rept 217. Commonwealth Scientific and Industrial Research Organisation, Australia.
- Phillips, B. F., and L. Olsen. 1975. The swimming behaviour of the puerulus stage of the western rock lobster. *Aust. J. Mar. Freshw. Res.* **26**: 415–417. doi:10.1071/MF9750415
- Phillips, B. F., D. W. Rimmer, and D. D. Reid. 1978. Ecological investigations of the late-stage phyllosoma and puerulus larvae of the western rock lobster *Panulirus longipes cygnus*. *Mar. Biol.* **45**: 347–357. doi:10.1007/BF00391821
- Phillips, B. F., J. D. Booth, J. S. Cobb, A. G. Jeffs, and P. McWilliam. 2006a. Larval and postlarval ecology, p. 231–262. *In* B. F. Phillips [ed.], *Lobsters: Biology, management, aquaculture and fisheries*. Blackwell.
- Phillips, B. F., A. G. Jeffs, R. Melville-Smith, C. F. Chubb, M. M. Nelson, and P. D. Nichols. 2006b. Changes in lipid and fatty acid composition of late larval and puerulus stages of the spiny lobster (*Panulirus cygnus*) across the continental shelf of Western Australia. *Comp. Biochem. Physiol. B Biochem. Mol. Biol.* **143**: 219–228. doi:10.1016/j.cbpb.2005.11.009
- Phillips, B. F., and P. S. McWilliam. 2009. Spiny lobster development: Where does successful metamorphosis to the puerulus occur?: A review. *Rev. Fish Biol. Fish.* **19**: 193–215. doi:10.1007/s11160-008-9099-5
- Rasband, W. S. 2015. ImageJ. U. S. National Institutes of Health. Accessed 13 June 2015. Available from <https://imagej.nih.gov/ij/>
- Richards, W. J., and T. Pothoff. 1981. Distribution and seasonal occurrence of larval pelagic stages of spiny lobsters (Palinuridae, *Panulirus*) in the western tropical Atlantic. *Proc. Gulf Carib. Fish. Inst.* **21**: 152–157.
- Rimmer, D. W., and B. F. Phillips. 1979. Diurnal migration and vertical distribution of phyllosoma larvae of the western rock lobster *Panulirus cygnus*. *Mar. Biol.* **54**: 109–124. doi:10.1007/BF00386590
- Ritz, D. A. 1972. Factors affecting the distribution of rock lobster larvae (*Panulirus longipes cygnus*), with reference to variability of plankton-net catches. *Mar. Biol.* **13**: 309–317. doi:10.1007/BF00348078
- Rutherford, A. 2001. *Introducing ANOVA and ANCOVA: A GLM approach*. SAGE Publications.
- Segura-García, I., L. Garavelli, M. Tringali, T. Matthews, L. M. Chérubin, J. Hunt, and S. J. Box. 2019. Reconstruction of larval origins based on genetic relatedness and biophysical modeling. *Sci. Rep.* **9**: 7100. doi:10.1038/s41598-019-43435-9
- Sekiguchi, H., and N. Inoue. 2002. Recent advances in larval recruitment processes of scyllarid and palinurid lobsters in Japanese waters. *J. Oceanogr.* **58**: 747–757. doi:10.1023/A:1022806726150
- Waite, A. M., and others. 2007. The Leeuwin Current and its eddies: An introductory overview. *Deep-Sea Res. II Top. Stud. Oceanogr.* **54**: 789–796. doi:10.1016/j.dsr2.2006.12.008
- Walker, J. M. 1994. The bicinchoninic acid (BCA) assay for protein quantitation, p. 5–8. *In* J. M. Walker [ed.], *Basic protein and peptide protocols*. Humana Press.
- Wang, M., R. O'Rorke, A. M. Waite, L. E. Beckley, P. Thompson, and A. G. Jeffs. 2014. Fatty acid profiles of phyllosoma larvae of western rock lobster (*Panulirus cygnus*) in cyclonic and anticyclonic eddies of the Leeuwin Current off Western Australia. *Prog. Oceanogr.* **122**: 153–162. doi:10.1016/j.pcean.2014.01.003
- Wilkin, J. L., and A. G. Jeffs. 2011. Energetics of swimming to shore in the puerulus stage of a spiny lobster: Can a post-larval lobster afford the cost of crossing the continental shelf? *Limnol. Oceanogr.: Fluids Environ.* **1**: 163–175. doi:10.1215/21573698-1504363
- Yeung, C., and M. F. McGowan. 1991. Differences in inshore-offshore and vertical distribution of phyllosoma larvae of *Panulirus*, *Scyllarus* and *Scyllarides* in the Florida Keys in May-June 1989. *Bull. Mar. Sci.* **49**: 699–714. doi:10.1071/MF01110
- Yeung, C., D. L. Jones, M. M. Criales, T. L. Jackson, and W. J. Richards. 2001. Influence of coastal eddies and counter-currents on the influx of spiny lobster, *Panulirus argus*, postlarvae into Florida Bay. *Mar. Freshw. Res.* **52**: 1217–1232. doi:10.1071/MF01110
- Yoshimura, T., H. Yamakawa, and E. Kozasa. 1999. Distribution of final stage phyllosoma larvae and free-swimming pueruli of *Panulirus japonicus* around the Kuroshio Current off southern Kyusyu, Japan. *Mar. Biol.* **133**: 293–306. doi:10.1007/s002270050468

Acknowledgments

We thank Captain L. Ríos-Mora and the crew of the R/V *Justo Sierra*, as well as C. A. Coronado-Méndez, I. Segura-García, J. P. Huchin-Mian,

R. Candia-Zulbarán, N. Herrera-Salvatierra, C. Flores-Cabrera, J. M. Ojeda-Cota, A. Almazán-Becerril, S. Escobar-Morales, S. Martínez-Gómez, and M. Ortiz-Matamoros, for their assistance during the oceanographic cruises. We also thank A. Jeffs, L. Zamora, and L. García Echaui at Leigh Marine Laboratory, University of Auckland for assistance with the biochemical analyses of pueruli. Funding for this study were provided by Universidad Nacional Autónoma de México (including the use of the R/V *Justo Sierra*) and Consejo Nacional de Ciencia y Tecnología (CONACYT, México) (Project No. 101200 granted to PBF). CONACYT also provided a Ph.D. scholarship for AFEM and M.Sc. scholarships for RMCH and RMC.

Conflict of Interest

None declared.

Submitted 24 September 2020

Revised 21 June 2021

Accepted 27 June 2021

Associate editor: James Leichter